

Self-induced parametric resonance in collective neutrino oscillations

Georg G. Raffelt¹

¹ *Max-Planck-Institut für Physik (Werner-Heisenberg-Institut), Föhringer Ring 6, 80805 München, Germany*
(Dated: 8 October 2008)

We identify a generic new form of collective flavor oscillations in dense neutrino gases that amounts to a self-induced parametric resonance. It occurs in a homogeneous and isotropic ensemble when a range of neutrino modes is prepared in a different flavor than the neighboring modes with lower and higher energies. The flavor content of the intermediate spectral part librates relative to the other parts with a frequency corresponding to a typical $\Delta m^2/2E$. This libration persists in the limit of an arbitrarily large neutrino density where one would have expected synchronized flavor oscillations.

PACS numbers: 14.60.Pq, 97.60.Bw

I. INTRODUCTION

Flavor oscillations in dense neutrino gases exhibit collective phenomena caused by neutrino-neutrino interactions [1, 2, 3, 4, 5, 6, 7, 8, 9, 10, 11, 12, 13, 14, 15, 16, 17, 18, 19, 20, 21, 22, 23, 24, 25, 26, 27, 28, 29, 30, 31, 32, 33, 34, 35, 36, 37, 38, 39, 40, 41, 42]. In the simplest example of a dense neutrino gas that is homogeneous and isotropic, studies of collective oscillations in the two-flavor context amount to solving the nonlinear equations of motion (EOMs) for a set of flavor polarization vectors \mathbf{P}_i ,

$$\dot{\mathbf{P}}_i = \mathbf{H}_i \times \mathbf{P}_i, \quad (1)$$

where

$$\mathbf{H}_i = \omega_i \mathbf{B} + \mu \mathbf{P}. \quad (2)$$

The “effective magnetic field” \mathbf{B} is a unit vector in flavor space and $\omega_i = \Delta m^2/2E_i$ the vacuum oscillation frequency for a neutrino mode with energy E_i . The total polarization vector of the ensemble is

$$\mathbf{P} = \sum_i \mathbf{P}_i. \quad (3)$$

Finally, $\mu \sim \sqrt{2} G_{\text{F}} n_\nu$ is a typical neutrino-neutrino interaction energy. Its exact definition depends on how we normalize the polarization vectors, but for our purpose it is simply an adjustable parameter of dimension energy.

Two main questions are of interest: What are the collective forms of motion in a dense neutrino gas? What happens when μ slowly decreases, mimicking the expanding universe or the neutrino density variation with distance from an astrophysical source? We concentrate on the former question and identify a new mode of collective oscillations that so far has gone unnoticed.

The simplest form of collective motion consists of “synchronized oscillations,” meaning that modes with different frequencies ω_i oscillate with a common frequency ω_{sync} if μ is sufficiently large [4, 6, 8]. The main physical idea is that the Hamiltonian vectors \mathbf{H}_i in Eq. (2) are dominated by $\mu \mathbf{P}$, forcing all \mathbf{P}_i to follow \mathbf{P} and thus to

a common precession around \mathbf{B} . It is this picture that we will see is not always complete.

Another case is the “pure precession mode” where each \mathbf{P}_i is collinear (parallel or antiparallel) to \mathbf{H}_i [27, 28, 29, 30]. Even though \mathbf{H}_i depends on all \mathbf{P}_i through \mathbf{P} , such a self-consistent solution exists for any strength of μ . All \mathbf{H}_i lie in the plane spanned by \mathbf{B} and \mathbf{P} . This plane rotates around \mathbf{B} , all \mathbf{P}_i being static within it. For $\mu \rightarrow \infty$ this solution requires all \mathbf{P}_i to be collinear and then is identical with a synchronized solution. Conversely, beginning with collinear \mathbf{P}_i and slowly reducing μ takes us adiabatically through different pure precession modes.

Finally, the “pendulum in flavor space” represents a class of solutions relevant for μ not too large [22, 24, 27]. The simplest case involves two vectors $\mathbf{P}_{1,2}$ that initially point in opposite directions. The dynamics of this system is equivalent to a gyroscopic pendulum. Once more, for $\mu \rightarrow \infty$ the motion is a common synchronized precession without nutation unless initially $\mathbf{P} = \mathbf{P}_1 + \mathbf{P}_2 = 0$.

It was always assumed that, unless initially $\mathbf{P} = 0$, the large- μ behavior is a synchronized precession. Likewise, it was assumed that the pure precession mode is stable. However, while a small perturbation may lead to small oscillations around the ideal solution, it may also lead to an exponential deviation. Numerical studies always found stable behavior for the pure precession mode and synchronized behavior in the large- μ limit. However, we will see that these findings depend on special choices of initial conditions and are not generic, although probably most relevant in the supernova context.

It is easy to see that the pure precession mode and its large- μ limit need not be stable. A pure precession mode with each \mathbf{P}_i collinear with \mathbf{H}_i is a self-consistent exact solution. Realistic initial conditions, however, begin with all \mathbf{P}_i collinear with each other, representing the assumption of all neutrinos being prepared in weak-interaction eigenstates. On the other hand, the initial μ may be large but must be finite. This initial condition is not an exact pure precession mode because each \mathbf{P}_i sports a small angle relative to its \mathbf{H}_i and thus moves on a precession cone with a small but nonzero opening angle. Therefore the total \mathbf{P} itself can not be static in

the co-rotating plane. Each \mathbf{P}_i precesses around \mathbf{H}_i with an approximate frequency μ , so \mathbf{P} itself must “vibrate” with a similar frequency.

We thus have a typical situation for a parametric resonance: Each \mathbf{P}_i precesses around \mathbf{H}_i with the approximate frequency μ and \mathbf{H}_i itself vibrates with a similar frequency. Therefore, while the precession cone of each \mathbf{P}_i follows its \mathbf{H}_i , it is not assured that the opening angle stays small. The exact outcome depends on how the evolution of the \mathbf{P}_i feeds back on \mathbf{P} and thus on \mathbf{H}_i .

To identify the simplest system showing such behavior we return to the EOMs of Eq. (1) and note that they have two exact invariants. One is the angular momentum along \mathbf{B} , so $\mathbf{B} \cdot \mathbf{P}$ is conserved [24]. The other is the energy [22, 25]

$$\mathbf{B} \cdot \mathbf{M} + \frac{\mu}{2} \mathbf{P}^2, \quad (4)$$

where the “total magnetic moment” is

$$\mathbf{M} = \sum_i \omega_i \mathbf{P}_i. \quad (5)$$

When $\mu \rightarrow \infty$ energy conservation implies that \mathbf{P}^2 and thus $|\mathbf{P}|$ are conserved [22]. \mathbf{P} then precesses around \mathbf{B} as a collective object, representing the usual synchronized oscillations.

This does not imply, however, that all \mathbf{P}_i remain collinear with \mathbf{P} . There can be internal motions among them such that $|\mathbf{P}|$ is conserved and \mathbf{P} still precesses as a collective object, yet the individual \mathbf{P}_i move relative to each other and relative to \mathbf{P} .

For two polarization vectors no internal motion is possible without modifying $|\mathbf{P}|$. Moreover, since $|\mathbf{P}_i|$ is conserved, the motion of each \mathbf{P}_i is described by two angles, so we have a total of four degrees of freedom. With two exact constants of the motion there remain two degrees of freedom, representing, for example, the “nutration angle” and the “precession angle” of the flavor pendulum. There is no room for new forms of motion.

If we have three or more polarization vectors that are initially aligned, nothing new happens either because the approximate conservation of $|\mathbf{P}|$ in the large- μ limit requires that the \mathbf{P}_i remain aligned.

Thus we need three polarization vectors (oscillation frequencies $\omega_1 < \omega_2 < \omega_3$), one of them initially anti-aligned with the others. If the “flipped” polarization vector is number 1 or 3 we are back to the flavor pendulum because in the large- μ limit two neighboring aligned vectors act roughly as one average mode. This is not possible if the flipped vector is number 2, so the relevant initial configuration is either up-down-up or down-up-down.

The main purpose of this paper is to study the most basic system of this sort and some simple generalizations. In Sec. II we solve analytically a very symmetric system consisting of three modes. In Sec. III we consider its counterpart for a continuous spectrum of modes and solve it analytically. We discuss the implications of our findings in Sec. IV.

II. THREE POLARIZATION VECTORS

A. Basic configuration

The basic configuration showing a self-induced parametric resonance consists of three polarization vectors with frequencies $\omega_1 < \omega_2 < \omega_3$. For simplicity we assume equal frequency spacings $\gamma = \omega_3 - \omega_2 = \omega_2 - \omega_1$. The common precession of the system around \mathbf{B} is irrelevant, so we can choose $\omega_2 = 0$, essentially going to a rotating frame around \mathbf{B} . The polarization vectors are $\mathbf{P}_{\pm,0}$ with oscillation frequencies $\pm\gamma$ and 0 and the EOMs are

$$\begin{aligned} \dot{\mathbf{P}}_{\pm} &= (\pm\gamma\mathbf{B} + \mu\mathbf{P}) \times \mathbf{P}_{\pm}, \\ \dot{\mathbf{P}}_0 &= \mu\mathbf{P} \times \mathbf{P}_0. \end{aligned} \quad (6)$$

Moreover, we assume that all polarization vectors have unit length and that initially \mathbf{P}_{\pm} point in the positive, \mathbf{P}_0 in the negative z -direction.

B. Numerical examples

We first illustrate the behavior of this system with a numerical example. We take \mathbf{B} to be tilted relative to the z -axis by an angle 2θ with $\cos 2\theta = 0.5$, θ itself playing the role of the neutrino mixing angle. In Fig. 1 we show the evolution of the projections of \mathbf{P}_{\pm} and \mathbf{P}_0 on \mathbf{P} for the interaction strength $\mu = 10\gamma$. The vector \mathbf{P}_0 evolves from its initial anti-alignment with \mathbf{P} to complete alignment and back, and so forth periodically. The other two vectors evolve similar to each other such that $\mathbf{B} \cdot \mathbf{P}$ is strictly conserved and the length $|\mathbf{P}|$ (uppermost curve) is approximately conserved.

The interesting internal evolution is relative to \mathbf{P} , so a large θ complicates the system by projection effects. We may use the opposite extreme of a vanishing θ because the existence of the new collective mode can not depend on this choice. A vanishing θ has the only disadvantage

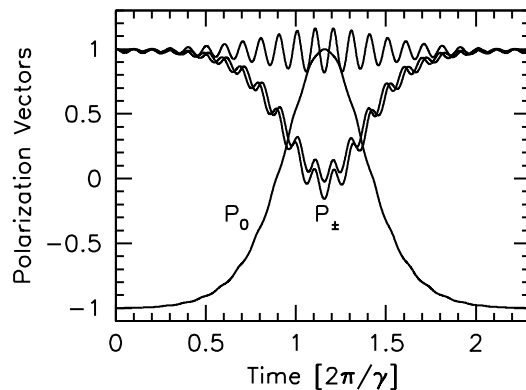


FIG. 1: Evolution of three polarization vectors for $\mu = 10\gamma$. We show \mathbf{P}_{\pm} and \mathbf{P}_0 , projected on the direction of the total \mathbf{P} . The uppermost curve is $|\mathbf{P}|$.

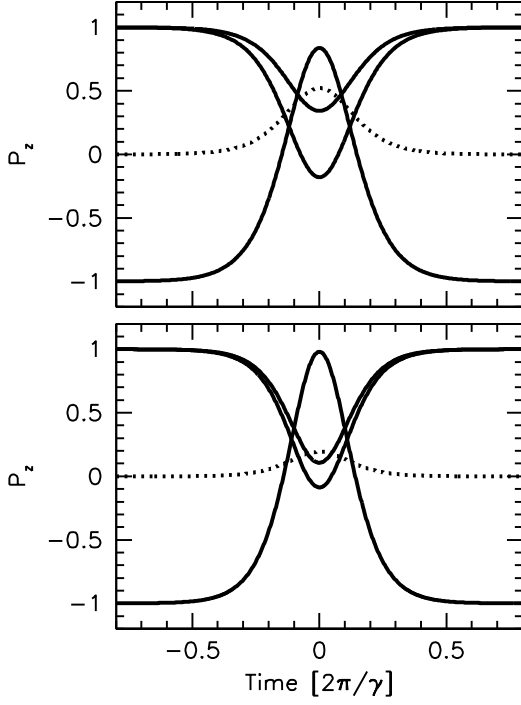


FIG. 2: Evolution of three polarization vectors as in Fig. 1, now with a small mixing angle and $\mu = 3\gamma$ (upper panel) and $\mu = 10\gamma$ (lower panel). The dotted line corresponds to the interaction energy (see text).

that the system can not start moving if the polarization vectors begin exactly collinear with \mathbf{B} . However, the motion can be excited by using a small but nonzero θ or by some other disturbance.

In Fig. 2 we show the evolution for an extremely small but nonzero mixing angle using $\mu = 3\gamma$ (upper panel) and $\mu = 10\gamma$ (lower panel). We do not show the long quasi-static phase where the system starts moving. One difference to the previous case is the absence of any “wiggles” even for a moderate μ . For larger μ the variation of the interaction energy $(\mu/2)\mathbf{P}^2$ becomes smaller. We show as a dotted line the quantity $(\mu/2)(\mathbf{P}^2 - 1)$. For $\mu \rightarrow \infty$ the two energy components $\mathbf{B} \cdot \mathbf{M}$ and $(\mu/2)\mathbf{P}^2$ seem to be separately conserved. It is striking that the “flipping time scale” remains the same.

We sketch the motion of the polarization vectors in Fig. 3. The vector \mathbf{P}_0 oscillates relative to \mathbf{P} , its relative orientation being described by the angle φ relative to the negative \mathbf{P} direction. If we use coordinates where the x -direction is defined by \mathbf{P}_0 we can describe the motion by the angle φ alone in the form

$$\mathbf{P}_0 = \begin{pmatrix} s \\ 0 \\ -c \end{pmatrix} \quad \text{and} \quad \mathbf{P}_{\pm} = \frac{1}{2} \begin{pmatrix} -s \\ \pm \sqrt{2(1-c)} \\ 1+c \end{pmatrix}, \quad (7)$$

where $s = \sin \varphi$ and $c = \cos \varphi$. In this way we always have $\mathbf{P} = (0, 0, 1)$. The energy components $\mathbf{B} \cdot \mathbf{M}$ and $(\mu/2)\mathbf{P}^2$ do not depend on φ .

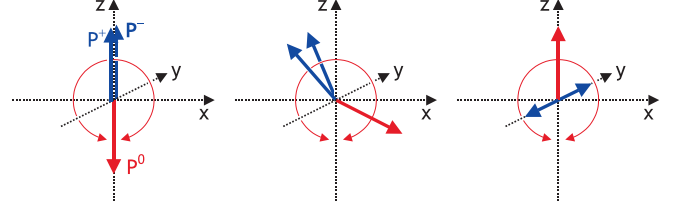


FIG. 3: Internal motion of three polarization vectors.

C. Analytic solution

Equation (7) must be a good approximation to the solutions of the EOMs, so all that is missing is the time evolution of φ . To find it we simplify the EOMs further and observe that the component of \mathbf{P} along \mathbf{B} is strictly conserved. Our choice of unit length for all vectors therefore implies $\mathbf{P} = \mathbf{B} + \mathbf{P}_{\perp}$ where \mathbf{P}_{\perp} is the \mathbf{P} component transverse to \mathbf{B} . Therefore, the EOMs are

$$\begin{aligned} \dot{\mathbf{P}}_{\pm} &= \mu \mathbf{P}_{\perp} \times \mathbf{P}_{\pm} + (\mu \pm \gamma) \mathbf{B} \times \mathbf{P}_{\pm}, \\ \dot{\mathbf{P}}_0 &= \mu \mathbf{P}_{\perp} \times \mathbf{P}_0 + \mu \mathbf{B} \times \mathbf{P}_0. \end{aligned} \quad (8)$$

We observe that there is a common precession with frequency μ around \mathbf{B} that represents the fast internal precession of all \mathbf{P}_i around \mathbf{P} . We can take out this common motion by going once more to a rotating frame so that finally the EOMs for the internal motion are

$$\begin{aligned} \dot{\mathbf{P}}_{\pm} &= \mu \mathbf{P}_{\perp} \times \mathbf{P}_{\pm} \pm \gamma \mathbf{B} \times \mathbf{P}_{\pm}, \\ \dot{\mathbf{P}}_0 &= \mu \mathbf{P}_{\perp} \times \mathbf{P}_0. \end{aligned} \quad (9)$$

We have achieved that fast precessions that are common to all polarization vectors have disappeared. The polarization vectors see the usual \mathbf{B} , leading to normal precessions, and in addition a transverse effective field represented by \mathbf{P}_{\perp} that tilts them.

This is analogous to the textbook example of magnetic resonance where an electron spin precesses fast in a strong external B field. Applying even the tiniest transverse B field that rotates with the original precession frequency leads to a situation where in the co-rotating frame the spin only feels the transverse component and completely reverses relative to the direction of the large external field.

In this example the rotation speed of the transverse B component must be adjusted to match the electron’s precession frequency. In our case this resonance condition arises automatically by the nonlinear nature of the problem where the transverse field is provided by the precessing polarization vectors themselves.

To solve the EOMs it is useful to introduce the difference vector

$$\mathbf{D} = \mathbf{P}_+ - \mathbf{P}_- \quad (10)$$

and study the motion of the three vectors \mathbf{P}_0 , \mathbf{D} and \mathbf{P}_{\perp} .

Their EOMs are

$$\dot{\mathbf{P}}_0 = \mu \mathbf{P}_\perp \times \mathbf{P}_0, \quad (11)$$

$$\dot{\mathbf{D}} = \mu \mathbf{P}_\perp \times \mathbf{D} + \gamma \mathbf{B} \times (\mathbf{P}_\perp - \mathbf{P}_0), \quad (12)$$

$$\dot{\mathbf{P}}_\perp = \gamma \mathbf{B} \times \left(\mathbf{D} - \frac{\mu}{\gamma} \mathbf{P}_\perp \right). \quad (13)$$

The vectors \mathbf{P}_0 and \mathbf{D} have lengths of order unity, whereas in the large- μ limit \mathbf{P}_\perp must be small. Energy conservation implies that it must be of order $(\gamma/\mu)^{1/2}$ or smaller. However, since \mathbf{P}_\perp appears on both the l.h.s. and r.h.s. of Eq. (13) and since it appears multiplied with μ on the r.h.s., both sides of this equation are of the same order in γ/μ only if to leading order

$$\mathbf{P}_\perp = \frac{\gamma}{\mu} \mathbf{D}. \quad (14)$$

Here we have assumed that to leading order \mathbf{D} has no component along \mathbf{B} because \mathbf{P}_+ and \mathbf{P}_- are expected to behave symmetrically. Inserting this into Eqs. (11) and (12) and neglecting terms of order γ/μ we find

$$\begin{aligned} \dot{\mathbf{P}}_0 &= \gamma \mathbf{D} \times \mathbf{P}_0, \\ \dot{\mathbf{D}} &= -\gamma \mathbf{B} \times \mathbf{P}_0. \end{aligned} \quad (15)$$

To leading order in γ/μ we have found a closed system of EOMs for \mathbf{P}_0 and \mathbf{D} alone. The strength of the neutrino-neutrino interaction has disappeared, only γ appears as an energy scale.

In our coordinate system \mathbf{P}_0 moves in the x - z plane whereas \mathbf{D} is along the y -direction. Describing the orientation of \mathbf{P}_0 with the angle φ as in Eq. (7), the EOMs finally become

$$\begin{aligned} \dot{\varphi} &= \gamma D, \\ \dot{D} &= -\gamma \sin \varphi. \end{aligned} \quad (16)$$

We recognize that φ and D play the role of canonically conjugate variables and that these EOMs follow from a Hamiltonian

$$H(\varphi, D) = \gamma \left[\frac{1}{2} D^2 + (\cos \varphi - 1) \right] \quad (17)$$

by virtue of $\dot{\varphi} = \partial H / \partial D$ and $\dot{D} = -\partial H / \partial \varphi$. Therefore, we have the EOM of a pendulum with frequency γ .

The initial condition \mathbf{P}_\pm aligned with \mathbf{B} and \mathbf{P}_0 anti-aligned corresponds to the initial condition $D = 0$ and $\varphi = 0$. In other words, the pendulum begins in an inverted position and obeys

$$\frac{\dot{\varphi}^2}{2} = \gamma^2 (1 - \cos \varphi). \quad (18)$$

This agrees well with numerical examples.

Using the vectors of Eq. (7) with any value φ_0 as an initial condition amounts to $D_0 = [2(1 - \cos \varphi_0)]^{1/2}$ or $\dot{\varphi}_0 = \gamma [2(1 - \cos \varphi_0)]^{1/2}$. The system follows the same solution (up to corrections of order γ/μ) for any φ_0 , except that the pendular motion begins in some phase of

the oscillation other than the inverted position. The pendulum begins with an initial excursion φ_0 and an initial velocity $\dot{\varphi}_0$, both adjusted such that it will reach the inverted position.

We can also choose other initial conditions with an arbitrary φ_0 and no initial velocity ($D_0 = 0$). In this case we have a pendulum that oscillates between two maximal excursion angles without reaching the inverted position. In terms of the polarization vectors this corresponds to \mathbf{P}_\pm being initially aligned with \mathbf{B} whereas \mathbf{P}_0 begins with a nonvanishing angle φ_0 .

We can choose this initial angle such that all three polarization vectors are initially almost aligned. In this case we obtain small-amplitude oscillations. This shows that our solution is also relevant for three initially aligned polarization vectors, the case where one finds synchronized oscillations. In the limit $\mu \rightarrow \infty$ and exactly aligned vectors nothing happens. However, for a finite μ and a small disturbance these vectors do oscillate. Here the small opening angles of the precession cones caused by the imperfect initial alignment between \mathbf{P}_i and \mathbf{H}_i also cause a parametric resonance, but in the direction of the small opening angles becoming smaller, then back to the original angle, and so forth. So the parametric resonance always occurs, but has a visible effect only if \mathbf{P}_0 is initially anti-aligned with \mathbf{P}_\pm .

We finally remark that the initial orientation of the three polarization vectors relative to \mathbf{B} is irrelevant. The initial conditions up-down-up or down-up-down are equivalent. In contrast to the gyroscopic flavor pendulum the neutrino mass hierarchy is here irrelevant.

D. Large mixing angle

We return to the case where \mathbf{P}_\pm and \mathbf{P}_0 are initially at some large angle 2θ relative to \mathbf{B} , corresponding to a large neutrino mixing angle θ . Armed with the insights gained in the previous section we note that we should study this situation in a coordinate system co-moving with \mathbf{P} and co-rotating with \mathbf{P}_0 around \mathbf{P} . Now the vector \mathbf{B} rotates with the large frequency μ around \mathbf{P} , its transverse component averaging to zero. In other words, we may consider the rotation-averaged EOMs in the same spirit as for the ordinary matter effect [22, 40].

The discussion of the previous section remains unchanged except that only the component of \mathbf{B} along \mathbf{P} contributes. This amounts to using the effective oscillation frequency $\gamma \cos 2\theta$. One can verify in numerical examples that this is indeed what happens. Even comparing our Figs. 1 and 2 reveals to the naked eye that a large θ value increases the oscillation period.

We conclude that the essential dynamics of our system does not depend on θ . For our theoretical study it is most convenient to use $\theta = 0$ whereas in numerical examples one uses a nonvanishing value that provides the necessary initial disturbance to start the motion.

E. Matter

Ordinary matter has the same effect on all modes and therefore can be removed by going into a rotating frame [22]. Since we anyway only study the internal motion of the \mathbf{P}_i and since we already go to a rotating frame to achieve this simplification, nothing new happens by the extra matter-induced rotation. Therefore, the effects discussed here are not modified by the presence of dense matter except for details of the initial disturbance caused by the fast-rotating \mathbf{B} .

F. Antineutrinos

Antineutrinos are most easily included in the EOMs as modes with negative frequencies $\omega = -|\Delta m^2/2E|$ [28], so in the most general case both neutrinos and antineutrinos are present. On the other hand, we constantly switch between rotating coordinate systems, shifting the zero-point of frequency at convenience. After each shift the behavior of the abstract system is the same, whereas its physical interpretation changes.

The polarization vectors used here are similar to the neutrino flavor isospin vectors of Duan et al. [22] in that for an antineutrino (negative frequency) “spin up” means $\bar{\nu}_\mu$ if for a neutrino (positive frequency) “spin up” means ν_e . Shifting between rotating coordinate systems therefore changes, for example, a $\bar{\nu}_\mu$ to a ν_e .

We repeat, however, that the interpretation of the polarization vectors is irrelevant with regard to the dynamics of the system. It is easiest to think of all modes as representing neutrinos in that any given distribution can be thought of as stemming from a neutrino distribution, suitably shifted to a rotating frame. Therefore, in an abstract discussion of the EOMs and their solutions, antineutrinos need not appear explicitly.

G. Fewer symmetries

We have studied a very symmetric system, but the general behavior persists if we vary the relative lengths of the vectors $\mathbf{P}_{\pm,0}$ and the frequency splittings. However, for any motion of this sort to be possible the three vectors must be able to move relative to each other while conserving \mathbf{P} . If \mathbf{P} is conserved, energy conservation implies that we also need to conserve $\mathbf{B} \cdot \mathbf{M}$.

Once the lengths of the three vectors are specified, their motion is described by two angles each, so a total of six angles. Our conditions provide four constraints, leaving two degrees of freedom: an irrelevant overall precession angle around \mathbf{P} and one angle describing the internal configuration.

The general conditions for a solution are not particularly illuminating, but we remark that, if \mathbf{P}_+ and \mathbf{P}_- have equal lengths, the parametric resonance requires $|\mathbf{P}_0| < 2|\mathbf{P}_\pm|$. This is verified in numerical examples.

III. SPECTRUM OF FREQUENCIES

A. Numerical Example

Next we consider a broad spectrum of modes. For convenience we scale all frequencies with a scale γ and use γt as a time coordinate, i.e., we use dimensionless frequencies. Without loss of generality we consider the range $-1 \leq \omega \leq +1$. We study the continuous generalization of the previous three-vector example, using an initial spectrum that is of box shape and has a flipped part in the middle (shaded spectrum in Fig. 4). We let this ensemble evolve with a fixed large μ , using a \mathbf{B} that is collinear with the polarization vectors except for a small mixing angle that triggers the motion. All modes oscillate with the same phase and reach their maximum excursion at the same time. We show the maximum excursion spectrum as a thick line in Fig. 4. The result is clearer when we “flip” the central part of the spectrum (dashed line). Within numerical accuracy, this compound curve is a Lorentzian resonance curve.

Therefore, the different parts of the neutrino spectrum librate relative to each other. In particular, the neutrinos with intermediate frequencies oscillate completely between two flavors with a typical vacuum oscillation frequency. The neutrino density does not enter as long as it is large in the sense $\mu \gg \gamma$.

We can make the “flipped” part of the spectrum narrower, obtaining a narrower Lorentzian. However, we can not make it arbitrarily broad in the same way as in the three-vector example the middle vector could not be longer than twice the length of the peripheral vectors. Here we find that the width of the flipped part must not exceed half the total box width. The transition is sharp in the sense that if the flipped part is slightly broader than half the total, nothing happens, if it is slightly smaller we find complete reversals and back of the central part of the spectrum.

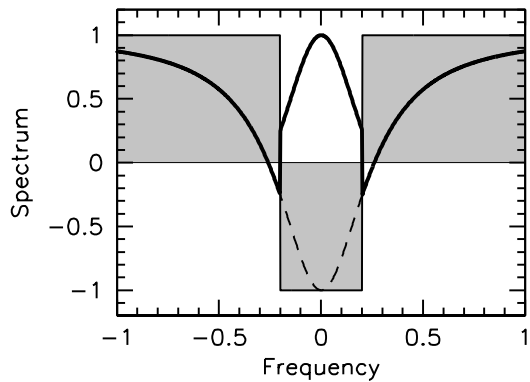


FIG. 4: Initial spectrum (thin line and shaded) and spectrum of maximum excursion (thick solid line), assuming a large fixed μ . The dashed line is the “flipped” version of the thick spectrum.

B. Analytic solution

To determine the exact solution in the large- μ limit we note that the EOMs in analogy to Eq. (9) are

$$\dot{\mathbf{P}}_\omega = \mu \mathbf{P}_\perp \times \mathbf{P}_\omega + \omega \mathbf{B} \times \mathbf{P}_\omega, \quad (19)$$

where each polarization vector is characterized by its frequency ω . We have assumed again that the mixing angle is small and therefore \mathbf{B} collinear with $\mathbf{P} = \int d\omega \mathbf{P}_\omega$. Integrating both sides over $\int d\omega$ leads to

$$\dot{\mathbf{P}}_\perp = \mathbf{B} \times (\mathbf{M} - \mu P \mathbf{P}_\perp) \quad (20)$$

where $P = |\mathbf{P}|$ is here not assumed to equal unity. The “magnetic moment” is $\mathbf{M} = \int d\omega \omega \mathbf{P}_\omega$. The same argument as in the three-vector example implies $\mathbf{P}_\perp = \mathbf{M}/(\mu P)$ to lowest order in μ^{-1} . We use spectra that are symmetric relative to $\omega = 0$ so that \mathbf{M} to lowest order has no component along \mathbf{B} . So the EOMs are

$$\dot{\mathbf{P}}_\omega = \left(\omega \mathbf{B} + \frac{\mathbf{M}}{P} \right) \times \mathbf{P}_\omega. \quad (21)$$

Once more we have eliminated the large frequency μ .

In this form it is clear that we expect a resonance shape of the oscillation pattern as a function of ω . Only the mode with $\omega = 0$ is exactly on resonance in that the transverse B field (here \mathbf{M}) is exactly co-rotating with it, or in our co-rotating coordinate system, does not move at all. The other modes precess around \mathbf{B} relative to the \mathbf{M} direction. They are not exactly on resonance.

For an explicit example we return to a box spectrum like Fig. 4 and define the function

$$s_\omega = \begin{cases} +1 & \text{for } \beta < |\omega| \leq 1, \\ -1 & \text{for } 0 \leq |\omega| \leq \beta. \end{cases} \quad (22)$$

The initial polarization vectors are

$$\mathbf{P}_\omega = \begin{pmatrix} 0 \\ 0 \\ s_\omega \end{pmatrix} \quad (23)$$

and so $P = |\mathbf{P}| = \int d\omega s_\omega = 2(1 - 2\beta)$. We further define the Lorentzian function

$$f_\omega = \frac{1}{(\omega/\Gamma)^2 + 1} \quad (24)$$

and fix its width by the condition

$$\int_{-1}^{+1} d\omega f_\omega s_\omega = 0 \quad (25)$$

which implies

$$\Gamma = \frac{\beta}{\sqrt{1 - 2\beta}}. \quad (26)$$

This is only possible for $\beta < \frac{1}{2}$, precisely the case where we find the parametric resonance.

As in the three-vector example we use a coordinate system where \mathbf{M} is oriented along the y direction and the oscillation of \mathbf{P}_0 takes place in the x - z plane. Once more we describe this vector by an angle φ such that

$$\mathbf{P}_0 = \begin{pmatrix} \sin \varphi \\ 0 \\ -\cos \varphi \end{pmatrix}. \quad (27)$$

Inspired by the numerical example and by the symmetries of our system we guess

$$\mathbf{P}_\omega = \left[\begin{pmatrix} 0 \\ 0 \\ 1 \end{pmatrix} - \begin{pmatrix} \sin \varphi \\ (\omega/\Gamma) \sqrt{2(1 - \cos \varphi)} \\ 1 - \cos \varphi \end{pmatrix} f_\omega \right] s_\omega. \quad (28)$$

Note that Eq. (25) and the symmetry of f_ω and s_ω guarantee that $\mathbf{P} = \int d\omega \mathbf{P}_\omega$ is the same for any φ .

Next we integrate Eq. (21) over $\int d\omega \omega$ so that on the r.h.s. the term $\mathbf{M} \times \mathbf{M}$ drops out and we find

$$\dot{\mathbf{M}} = \mathbf{B} \times \int d\omega \omega^2 \mathbf{P}_\omega. \quad (29)$$

The vector \mathbf{M} has only a y -component that is found to be $\Gamma P \sqrt{2(1 - \cos \varphi)}$. The vector on the r.h.s. also has only a y -component $\Gamma^2 P \sin \varphi$. Therefore, once more the excursion angle evolves like an inverted pendulum,

$$\dot{\varphi} = \Gamma \sqrt{2(1 - \cos \varphi)}. \quad (30)$$

It is now easy to verify that Eq. (28) indeed solves the EOMs of Eq. (21).

C. Single-crossed spectrum

The behavior found in the previous section is similar for less symmetric arrangements. However, the “flipped” part of the spectrum must not be too broad and must not get too close to the edges of the overall box. In other words, the two “wings” of the spectrum must be large enough to support the parametric resonance, but we have not worked out the general condition.

The crucial feature is to have a “double-crossed” spectrum $s(\omega)$, representing the initial z -component of \mathbf{P}_ω . The spectrum must first cross from positive to negative and then back to positive values or the other way round. One can also construct multiple-crossed spectra and finds more complicated parametric resonance patterns.

On the other hand, this form of collective motion can not occur for a single-crossed spectrum where $s(\omega) < 0$ for $\omega < \omega_{\text{cross}}$ and $s(\omega) > 0$ for $\omega > \omega_{\text{cross}}$. Here $\mathbf{B} \cdot \mathbf{M}$ is maximal, so moving any polarization vector makes it smaller. This is easily seen if we go to a rotating frame where $\omega_{\text{cross}} = 0$. This has the effect $\mathbf{B} \cdot \mathbf{M} = \mathbf{B} \cdot \sum_i \omega_i \mathbf{P}_i \rightarrow \mathbf{B} \cdot \sum_i (\omega_i - \omega_{\text{cross}}) \mathbf{P}_i = \mathbf{B} \cdot \mathbf{M} - \omega_{\text{cross}} \mathbf{B} \cdot \mathbf{P}$ and since $\mathbf{B} \cdot \mathbf{P}$ is a constant of the motion, we have only added a constant term to the energy. In the new system with $\omega_{\text{cross}} = 0$ all modes with negative frequencies get

multiplied with a negative $s(\omega)$, the positive ones with a positive $s(\omega)$. Therefore, any motion of \mathbf{P}_ω lowers $\mathbf{B} \cdot \mathbf{M}$. The opposite is true if the spectrum crosses from positive to negative values or if we take \mathbf{B} to point in the negative z -direction. In other words, even though for a single-crossed spectrum one could move the polarization vectors such that $|\mathbf{P}|$ and $(\mu/2)\mathbf{P}^2$ remain unchanged, the quantity $\mathbf{B} \cdot \mathbf{M}$ is extremal.

A single-crossed spectrum is the prototype for a gyroscopic flavor pendulum that is driven by the exchange of energy between $(\mu/2)\mathbf{P}^2$ (playing the role of kinetic energy) and $\mathbf{B} \cdot \mathbf{M}$ (potential energy). In the large- μ limit the oscillations are synchronized and, if the mixing angle is small, nothing visible happens.

If one assumes that a source only emits neutrinos and antineutrinos of one flavor, e.g. a flux of ν_e (positive ω) together with a flux of $\bar{\nu}_e$ (negative ω) one has a single-crossed spectrum in that the polarization vectors for ν_e are “spin up,” those for $\bar{\nu}_e$ “spin down” as explained in Sec. II F. Therefore, in this situation the parametric resonance does not play any role.

D. Nonisotropic system

The parametric resonance is probably not possible if the neutrino ensemble is not isotropic. Assuming axial symmetry around some direction we can describe every mode by its frequency ω and the velocity projection v on the symmetry axis. The EOMs are in this case [23, 25]

$$\dot{\mathbf{P}}_{\omega,v} = \mathbf{H}_{\omega,v} \times \mathbf{P}_{\omega,v}, \quad (31)$$

where

$$\mathbf{H}_{\omega,v} = \omega \mathbf{B} + \mu(\mathbf{P} - v\mathbf{F}) \quad (32)$$

and

$$\mathbf{P} = \int d\omega dv \mathbf{P}_{\omega,v}, \quad \mathbf{F} = \int d\omega dv v \mathbf{P}_{\omega,v}. \quad (33)$$

Even if the vectors \mathbf{P} and \mathbf{F} are collinear, there is no longer a co-rotating frame where all polarization vectors would see essentially the same effective magnetic field. If one of them were on resonance with regard to some transverse field, the others would precess with different angular velocities where the differences are much larger than order ω in the large- μ limit.

We have studied a few numerical examples where we assumed a homogeneous ensemble with a “half-isotropic” distribution, i.e., all modes with velocity components in the positive direction of the symmetry axis were isotropically occupied, those with negative velocity components were taken to be empty. The parametric resonance indeed disappeared for all tested examples where it occurred in the corresponding isotropic case.

IV. DISCUSSION

We have shown that in a dense neutrino gas, neutrino-neutrino interactions can lead to a parametric resonance that causes different parts of the flavor spectrum to oscillate relative to each other. This effect persists in the large-density limit where one would have expected synchronized oscillations. The new pattern is an internal motion among the ensemble of polarization vectors that still precess together as a collective object, but do not retain a common orientation relative to each other. The strength of the neutrino-neutrino interaction does not appear in the oscillation frequency that is determined entirely by the spectrum of vacuum oscillation frequencies.

However, the parametric resonance has a macroscopic impact only if the initial flavor spectrum $s(\omega)$ is at least “double crossed” in that there must be a spectral flavor sequence of the form up-down-up or the other way round. We use polarization vectors similar to “neutrino flavor isospin vectors” where, for example, a $\bar{\nu}_e$ mode is “spin down” if ν_e is defined as “spin up.” Therefore, a neutrino flux initially consisting of neutrinos and antineutrinos of a single flavor represents a single-crossed case: $s(\omega)$ changes sign once at $\omega = 0$ going from antineutrinos to neutrinos. Most numerical studies of supernova neutrino oscillations used such single-crossed spectra and the parametric resonance did not show up.

A dense gas of neutrinos and antineutrinos of different flavors in kinetic (but not chemical) equilibrium is also single crossed. For a Fermi-Dirac distribution the spectral shape and amplitude are fixed by the temperature and chemical potential. If the distributions for two flavors are described by the same T but different degeneracy parameters, they do not cross. Our spectrum $s(\omega)$ with $\omega = \Delta m^2/2E$ represents the difference between the distributions of the two flavors because the identical parts drop out of the oscillation equations. The only crossing occurs at $\omega = 0$ at the spectral junction between antineutrinos and neutrinos.

Flavor-dependent neutrino chemical potentials are important inside a supernova core and also in the early universe if primordial neutrino asymmetries exist. The usual picture of synchronized oscillations and/or a synchronized MSW resonance remains unchanged. In this context the parametric resonance apparently does not lead to a novel speed-up of flavor conversions.

Neutrinos streaming from a supernova core are not black-body radiation. Even if one approximates the fluxes of ν_e , $\bar{\nu}_e$ and the other species by Fermi-Dirac distributions, the effective temperatures and chemical potentials are different. Typically one finds three spectral crossings, the usual one at $\omega = 0$ and one for a negative and one for a positive ω , see for example Ref. [32]. However, neutrinos streaming from a source are strongly anisotropic, so the parametric resonance would be suppressed by multi-angle effects as discussed in Sec. III D even if the spectral conditions were appropriate.

Therefore, it is unclear if the collective motion rep-

resented by the parametric resonance is realized in any practical astrophysical or cosmological context. Perhaps the main insight is that even for a slowly changing or fixed μ the individual polarization vectors \mathbf{P}_i need not follow their “single-particle Hamiltonians” \mathbf{H}_i even if the system as a whole evolves adiabatically.

In the supernova context one is primarily concerned with the fate of flavor-dependent neutrino spectra as a function of radius, the decreasing neutrino-neutrino interaction producing a “spectral split.” In the homogeneous and isotropic model represented by Eq. (1) this occurs if μ slowly decreases so that \mathbf{H}_i changes from being $\mu\mathbf{P}$ -dominated to being $\omega_i\mathbf{B}$ -dominated. For a single-crossed spectrum the occurrence of a split is explained by each \mathbf{P}_i following its \mathbf{H}_i in the co-rotating frame. The spectral split occurs at a frequency ω_{split} corresponding to the final co-rotation frequency. Its value can be found from the conservation of $\mathbf{B} \cdot \mathbf{P}$. In the present case of a double-crossed spectrum a slowly decreasing μ leads to two spectral splits. Multiple-crossed spectra lead to multiple spectral splits. The occurrence of multiple splits is not directly accounted for by the picture of all \mathbf{P}_i following their \mathbf{H}_i in a single co-rotating frame and a full theoretical understanding of the phenomenon of multiple spectral splits is presently missing.

The parametric resonance and multiple splits are not directly related even though this investigation was motivated by the numerical observation of multiple splits. A parametric resonance for our box-spectrum requires the flipped middle part not to exceed half the box width

whereas a double split occurs for any width of the flipped part. It is actually surprising that the large- μ oscillations have no apparent impact on the final sharp double-split that is found in the adiabatic limit of a slowly decreasing μ . One also finds that multiple splits are not, or at least not always, prevented by multi-angle effects for neutrinos streaming from a source. On the other hand, the collective motion found here is “fragile” and easily suppressed by multi-angle effects as explained earlier.

Perhaps the main lesson from our investigation is that the innocent-looking EOMs of Eq. (1) continue to surprise us with unexpected solutions, even if these solutions need not be of direct astrophysical relevance. Much of the insights gained about collective neutrino oscillations are owed to “numerical experiments” followed in some cases by theoretical explanations and even analytic solutions. One may well worry if our current understanding of these nonlinear equations is sufficiently advanced to arrive at robust conclusions about possible observable effects for example in supernova neutrino spectra. More theoretical work may well turn up more surprises.

Acknowledgements

This work was partly supported by the Deutsche Forschungsgemeinschaft under grant TR-27 “Neutrinos and Beyond” and the Cluster of Excellence “Origin and Structure of the Universe” (Munich and Garching).

-
- [1] J. Pantaleone, “Neutrino oscillations at high densities,” *Phys. Lett. B* **287**, 128 (1992).
 - [2] J. Pantaleone, “Stability of incoherence in an isotropic gas of oscillating neutrinos,” *Phys. Rev. D* **58**, 073002 (1998).
 - [3] G. Sigl and G. Raffelt, “General kinetic description of relativistic mixed neutrinos,” *Nucl. Phys. B* **406**, 423 (1993).
 - [4] S. Samuel, “Neutrino oscillations in dense neutrino gases,” *Phys. Rev. D* **48**, 1462 (1993).
 - [5] V. A. Kostecký and S. Samuel, “Neutrino oscillations in the early universe with an inverted neutrino mass hierarchy,” *Phys. Lett. B* **318**, 127 (1993).
 - [6] V. A. Kostecký and S. Samuel, “Self-maintained coherent oscillations in dense neutrino gases,” *Phys. Rev. D* **52**, 621 (1995) [hep-ph/9506262].
 - [7] S. Samuel, “Bimodal coherence in dense selfinteracting neutrino gases,” *Phys. Rev. D* **53**, 5382 (1996) [hep-ph/9604341].
 - [8] S. Pastor, G. G. Raffelt and D. V. Semikoz, “Physics of synchronized neutrino oscillations caused by self-interactions,” *Phys. Rev. D* **65**, 053011 (2002) [hep-ph/0109035].
 - [9] A. D. Dolgov, S. H. Hansen, S. Pastor, S. T. Petcov, G. G. Raffelt and D. V. Semikoz, “Cosmological bounds on neutrino degeneracy improved by flavor oscillations,” *Nucl. Phys. B* **632**, 363 (2002) [arXiv:hep-ph/0201287].
 - [10] Y. Y. Y. Wong, “Analytical treatment of neutrino asymmetry equilibration from flavour oscillations in the early universe,” *Phys. Rev. D* **66**, 025015 (2002) [hep-ph/0203180].
 - [11] K. N. Abazajian, J. F. Beacom and N. F. Bell, “Stringent constraints on cosmological neutrino antineutrino asymmetries from synchronized flavor transformation,” *Phys. Rev. D* **66**, 013008 (2002) [astro-ph/0203442].
 - [12] S. Pastor, T. Pinto and G. Raffelt, “Relic density of neutrinos with primordial asymmetries,” arXiv:0808.3137.
 - [13] S. Pastor and G. Raffelt, “Flavor oscillations in the supernova hot bubble region: Nonlinear effects of neutrino background,” *Phys. Rev. Lett.* **89**, 191101 (2002) [astro-ph/0207281].
 - [14] R. F. Sawyer, “Classical instabilities and quantum speed-up in the evolution of neutrino clouds,” hep-ph/0408265.
 - [15] R. F. Sawyer, “Speed-up of neutrino transformations in a supernova environment,” *Phys. Rev. D* **72**, 045003 (2005) [hep-ph/0503013].
 - [16] R. F. Sawyer, “The multi-angle instability in dense neutrino systems,” arXiv:0803.4319.
 - [17] N. F. Bell, A. A. Rawlinson and R. F. Sawyer, “Speed-up through entanglement: Many-body effects in neutrino processes,” *Phys. Lett. B* **573**, 86 (2003) [hep-ph/0304082].
 - [18] A. Friedland and C. Lunardini, “Do many-particle neutrino interactions cause a novel coherent effect?,” *JHEP*

- 0310**, 043 (2003) [hep-ph/0307140].
- [19] A. Friedland and C. Lunardini, “Neutrino flavor conversion in a neutrino background: Single- versus multi-particle description,” *Phys. Rev. D* **68**, 013007 (2003) [hep-ph/0304055].
 - [20] A. Friedland, B. H. J. McKellar and I. Okuniewicz, “Construction and analysis of a simplified many-body neutrino model,” *Phys. Rev. D* **73**, 093002 (2006) [hep-ph/0602016].
 - [21] A. B. Balantekin and Y. Pehlivan, “Neutrino neutrino interactions and flavor mixing in dense matter,” *J. Phys. G* **34**, 47 (2007) [astro-ph/0607527].
 - [22] H. Duan, G. M. Fuller and Y. Z. Qian, “Collective neutrino flavor transformation in supernovae,” *Phys. Rev. D* **74**, 123004 (2006) [astro-ph/0511275].
 - [23] H. Duan, G. M. Fuller, J. Carlson and Y. Z. Qian, “Simulation of coherent non-linear neutrino flavor transformation in the supernova environment. I: Correlated neutrino trajectories,” *Phys. Rev. D* **74**, 105014 (2006) [astro-ph/0606616].
 - [24] S. Hannestad, G. G. Raffelt, G. Sigl and Y. Y. Y. Wong, “Self-induced conversion in dense neutrino gases: Pendulum in flavor space,” *Phys. Rev. D* **74**, 105010 (2006); Erratum *ibid.* **76**, 029901 (2007) [astro-ph/0608695].
 - [25] G. G. Raffelt and G. Sigl, “Self-induced decoherence in dense neutrino gases,” *Phys. Rev. D* **75**, 083002 (2007) [hep-ph/0701182].
 - [26] A. Esteban-Pretel, S. Pastor, R. Tomàs, G. G. Raffelt and G. Sigl, “Decoherence in supernova neutrino transformations suppressed by deleptonization,” *Phys. Rev. D* **76**, 125018 (2007) [arXiv:0706.2498].
 - [27] H. Duan, G. M. Fuller, J. Carlson and Y. Z. Qian, “Analysis of collective neutrino flavor transformation in supernovae,” *Phys. Rev. D* **75**, 125005 (2007) [astro-ph/0703776].
 - [28] G. G. Raffelt and A. Yu. Smirnov, “Self-induced spectral splits in supernova neutrino fluxes,” *Phys. Rev. D* **76**, 081301 (2007); Erratum *ibid.* **77**, 029903 (2008) [arXiv:0705.1830].
 - [29] G. G. Raffelt and A. Yu. Smirnov, “Adiabaticity and spectral splits in collective neutrino transformations,” *Phys. Rev. D* **76**, 125008 (2007) [arXiv:0709.4641].
 - [30] H. Duan, G. M. Fuller and Y. Z. Qian, “A simple picture for neutrino flavor transformation in supernovae,” *Phys. Rev. D* **76**, 085013 (2007) [arXiv:0706.4293].
 - [31] H. Duan, G. M. Fuller, J. Carlson and Y. Z. Qian, “Neutrino mass hierarchy and stepwise spectral swapping of supernova neutrino flavors,” *Phys. Rev. Lett.* **99**, 241802 (2007) [arXiv:0707.0290].
 - [32] G. L. Fogli, E. Lisi, A. Marrone and A. Mirizzi, “Collective neutrino flavor transitions in supernovae and the role of trajectory averaging,” *JCAP* **0712**, 010 (2007) [arXiv:0707.1998].
 - [33] G. L. Fogli, E. Lisi, A. Marrone, A. Mirizzi and I. Tamborra, “Low-energy spectral features of supernova (anti) neutrinos in inverted hierarchy,” arXiv:0808.0807.
 - [34] H. Duan, G. M. Fuller, J. Carlson and Y. Z. Qian, “Flavor evolution of the neutronization neutrino burst from an O-Ne-Mg core-collapse supernova,” *Phys. Rev. Lett.* **100**, 021101 (2008) [arXiv:0710.1271].
 - [35] B. Dasgupta, A. Dighe, A. Mirizzi and G. G. Raffelt, “Spectral split in prompt supernova neutrino burst: Analytic three-flavor treatment,” *Phys. Rev. D* **77**, 113007 (2008) [arXiv:0801.1660].
 - [36] A. Esteban-Pretel, S. Pastor, R. Tomàs, G. G. Raffelt and G. Sigl, “Mu-tau neutrino refraction and collective three-flavor transformations in supernovae,” *Phys. Rev. D* **77**, 065024 (2008) [arXiv:0712.1137].
 - [37] B. Dasgupta and A. Dighe, “Collective three-flavor oscillations of supernova neutrinos,” *Phys. Rev. D* **77**, 113002 (2008) [arXiv:0712.3798].
 - [38] H. Duan, G. M. Fuller and Y. Z. Qian, “Stepwise spectral swapping with three neutrino flavors,” *Phys. Rev. D* **77**, 085016 (2008) [arXiv:0801.1363].
 - [39] B. Dasgupta, A. Dighe and A. Mirizzi, “Identifying neutrino mass hierarchy at extremely small θ_{13} through Earth matter effects in a supernova signal,” arXiv:0802.1481.
 - [40] A. Esteban-Pretel, A. Mirizzi, S. Pastor, R. Tomàs, G. G. Raffelt, P. D. Serpico and G. Sigl, “Role of dense matter in collective supernova neutrino transformations,” *Phys. Rev. D*, in press (2008) [arXiv:0807.0659].
 - [41] S. Chakraborty, S. Choubey, B. Dasgupta and K. Kar, “Effect of collective flavor oscillations on the diffuse supernova neutrino background,” *JCAP* **0809**, 013 (2008) [arXiv:0805.3131].
 - [42] J. Gava and C. Volpe, “Collective neutrino oscillations in matter and CP-violation,” arXiv:0807.3418.